# Technical and economic analysis of wet compression–resorption heat pumps

Gudjonsdottir, V.; Infante Ferreira, C. A.

**DOI**
10.1016/j.ijrefrig.2020.05.010

**Publication date**
2020

**Document Version**
Final published version

**Published in**
International Journal of Refrigeration

International Journal of Refrigeration 117 (2020) 140–149

Contents lists available at ScienceDirect

International Journal of Refrigeration

journal homepage: www.elsevier.com/locate/ijrefrig

# Technical and economic analysis of wet compression–resorption heat pumps

V. Gudjonsdottir*, C.A. Infante Ferreira

*Process and Energy Laboratory, Delft University of Technology, Leeghwaterstraat 39, 2628 CB, Delft, The Netherlands*

ARTICLE INFO

*Article history:*
Received 20 January 2020
Revised 26 April 2020
Accepted 12 May 2020
Available online 20 May 2020

*Keywords:*
High temperature heat pumps
$NH_3$–$CO_2$–$H_2O$
$NH_3$-$H_2O$
Twin-screw compressor
Technical and economic analysis

ABSTRACT

Heat pumps can efficiently upgrade waste heat from the industry and in that way reduce emissions. One of the main reasons why heat pumps are not applied to a greater extent in industry are large payback periods. Compression–resorption heat pumps (CRHP) enhanced by wet compression are considered a very promising option that can have higher coefficient of performance compared to traditional technologies when the heat source and/or sink have a large temperature glide. In this study the thermodynamic and economic performance of two potential industrial cases are examined for CRHP operating with $NH_3$–$H_2O$ and $NH_3$–$CO_2$–$H_2O$. A detailed thermodynamic model of the compressor is used to evaluate the isentropic efficiency for each case. The results are used to calculate the simple payback period, when a boiler is replaced by a CRHP, as a function of the predicted gas and electricity prices in the Netherlands from 2020 to 2035. The results indicate that adding $CO_2$ to the $NH_3$–$H_2O$ mixture increases the cycle COP when the temperature glide of the heat sink is 40 K while the opposite occurs when the glide is 80 K. The highest COPs and lowest payback times are obtained when the outlet vapor quality is around 0.50 for both the binary and ternary mixtures. Larger glides require higher outlet qualities. However, it is clear that even for high temperature glides the payback period can be within acceptable limits, especially if the cost of $CO_2$ emissions is taken into account.



# Analyse technique et économique des pompes à chaleur à compression-résorption humide

*Mots-clés:* Pompes à chaleur à haute température; NH-CO-HO; NH-HO; Compresseur à double vis; Analyse technique et économique

## 1. Introduction

Heat pumps have the potential to reduce dramatically the use of expensive utilities in the process industry, with significant energy savings and associated major reduction in GHG emissions (Kiss and Infante Ferreira, 2016). However, the actual use of heat pumps in the industry is still rather limited. According to the International Energy Agency one of the main reasons is long payback periods, often in the range of 5–8 years or even more (IEA, 2014).

In recent years various review articles investigated industrial heat pumps. For instance, Zhang et al. (2016) reviewed the applications of industrial heat pumps in China. Bamigbetan et al. (2017) as well as Arpagaus et al. (2018) reviewed high temperature heat pumps (HTHP), and Arpagaus et al. (2016) multi-temperature heat pumps. As Bamigbetan et al. (2017) mention, the vapor compression cycle (VCHP) is the most widely used heat pump concept. Many research directions have been taken to improve its performance, including investigation of alternative refrigerants, cascade systems and 2-stage cycles. Furthermore, other heat pump systems have been considered such as absorption heat pumps and hybrid heat pumps. For many applications, where there is a temperature glide of the heat sink and/or the heat source, compression–resorption heat pumps (CRHP) are a very promising option, especially when using wet compression. That is, staying in the two phase region during the entire compression process. In this way

* Corresponding author.
*E-mail address:* vilborgg1@gmail.com (V. Gudjonsdottir).

https://doi.org/10.1016/j.ijrefrig.2020.05.010

**Nomenclature**

| | |
|---|---|
| $c$ | Specific energy cost € $kWh^{-1}$ |
| $CRF$ | Capital recovery factor |
| $FC$ | Annual fuel consumption cost € |
| $H$ | Yearly operating time h |
| $h$ | Specific enthalpy J $kg^{-1}$ |
| $i$ | Interest rate |
| $i_L$ | Inflation rate |
| $m$ | Mass kg |
| $OMC$ | Operation and maintenance cost € |
| $P$ | Pressure Pa |
| $PBP$ | Payback period years |
| $PEC$ | Purchased Equipment Cost € |
| $Q$ | Heat J |
| $q$ | Vapor quality |
| $\dot{Q}$ | Heat duty W |
| $s$ | Specific entropy J $kg^{-1}$ $K^{-1}$ |
| $T$ | Temperature K |
| $TCI$ | Total Capital Investment € |
| $V$ | Volume $m^3$ |
| $v$ | Specific volume $m^3$ $kg^{-1}$ |
| $\dot{V}$ | Volumetric flow $m^3$ $s^{-1}$ |
| $X$ | Component size or capacity |
| $x$ | Mass concentration kg $kg^{-1}$ |

*Greek Symbols*

| | |
|---|---|
| $\Delta$ | Difference |
| $\eta$ | Efficiency |
| $\gamma$ | Cost function exponent |
| $\phi$ | Male rotor turning angle |
| $\rho$ | Density kg $m^{-3}$ |

*Sub and superscripts*

| | |
|---|---|
| 2st | 2 stage |
| avg | Average |
| comb | Combined |
| comp | Compressor |
| cw | Waste heat stream |
| des | Desorber |
| driving | Driving |
| eff | Effective |
| el | Electricity |
| high | Higher |
| HP | Heat Pump |
| in | Inlet |
| interm | Intermediate |
| is | Isentropic (total) |
| low | Lower |
| LT | Technical life time years |
| motor | Motor |
| NG | Natural Gas |
| out | Outlet |
| res | Resorber |
| s | Isentropic |
| vol | Volumetric |
| W | Equipment with known cost |
| Y | Equipment with calculated cost |

*Abbreviations*

| | |
|---|---|
| COP | Coefficient of Performance |
| CRHP | Compression–resorption heat pumps |
| ECN | Energy research Center of the Netherlands |
| GHG | Green house gas |
| GWP | Global warming potential |
| HTHP | High temperature heat pumps |
| VCHP | Vapor compression heat pumps |

the superheating at the compressor outlet is eliminated and the heat sink can be upgraded to higher values.

Lately an increased interest has been on HTHP, defined as delivering heat above 100 °C by Arpagaus et al. (2018). This is for a good reason. Arpagaus et al. (2018) estimate the technical potential for industrial heat pumps, delivering process heat in the range 100–150 °C, in Europe to be 113 PJ. There are several limitations when it concerns HTHP. One of the main challenges is to find a suitable high temperature working fluid that has a low global warming potential (GWP). The main working fluids that have been applied in HTHP are R245fa, R717 (ammonia), R744 ($CO_2$), R134a, and R1234ze(E) (Arpagaus et al., 2018). Both R134a and R245fa have a high global warming potential of 1300 and 858, respectively. Some studies have been conducted to find low GWP alternatives, in all cases only pure refrigerants have been researched (Fukuda et al., 2014; Kondou and Koyama, 2015; Mikielewicze and Wajs, 2019). Limited number of studies have looked at mixtures for high temperature applications and in two recent cases the thermodynamic properties are not reported (Xiaohui et al., 2014; Zhang et al., 2017). Both water and ammonia have 0 GWP. One of the main problems of operating a heat pump with water is that the vapor density is very low, resulting in high volume flows. Additionally, the lower pressure level can be significantly below atmospheric pressure. On the other hand when operating with ammonia special high pressure equipment is needed at high temperatures, resulting in additional costs. Similarly, operating a heat pump with $CO_2$, with a GWP of 1, the operating pressures are high. Operating a CRHP with an $NH_3$–$H_2O$ mixture or $NH_3$–$CO_2$–$H_2O$ can solve the low and high pressure problems. By choosing the mixture concentration carefully the operating pressures can stay within reasonable limits. Additionally, as mentioned above, by utilizing wet compression, high temperatures can easily be reached.

Several experiments have been performed using liquid injection during the vapor compression process with good results (Cao et al., 2011; Shen et al., 2016; Tian et al., 2017). However, limited studies have been performed with wet compression and a commercial solution of such a compressor is not available, to the best of the authors'knowledge. If such a compressor becomes available then considerable advantages can be obtained with CRHP as compared to traditional technologies. The achieved payback periods could be shortened significantly compared to traditional technologies, especially for applications with temperature glides and high temperature lifts (van de Bor and Infante Ferreira, 2013).

Additionally, with the increasing $CO_2$ emission allowance price the payback periods for heat pumps can improve significantly. The price set by the European Union Emission Trading System has increased dramatically in the recent years with a jump of around 200% in 2018 alone (Król and Oclon, 2019) and it has kept on increasing in 2019. This has been a much steeper increase than predicted by, for example, ECN in 2017 (ECN, 2017). They predicted that the price would be around 7 € $ton^{-1}$ $CO_2$ in 2020 and not go up to 25 € $ton^{-1}$ $CO_2$ until 2035, which it has already reached in 2019. This increase is positive news for heat pumps that can, as mentioned at the beginning of the introduction, significantly reduce $CO_2$ emissions in industry.

This study investigates two industrial CRHP systems using wet compression, thermodynamically and economically. Different from previous studies, the isentropic and volumetric efficiencies of the compressor are determined for each operating condition by a dedicated compressor model. Additionally, the manuscript investigates the performance of binary $NH_3$–$H_2O$ systems and also ternary

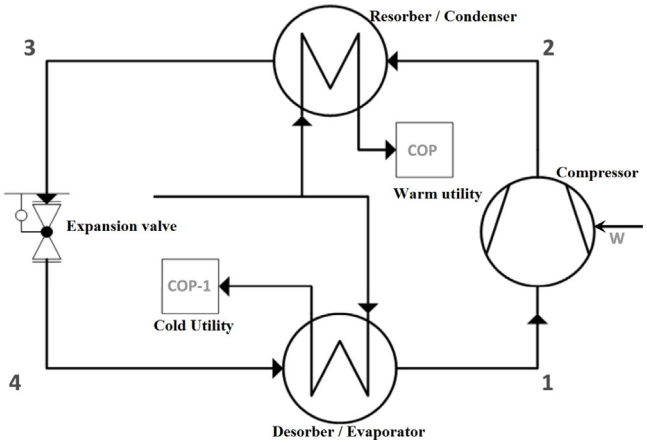


**Fig. 1.** A schematic of a heat pump; splitting a waste heat stream into a warm and cold utility stream. Compared to VCHP, the condenser is replaced by a resorber and the evaporator by a desorber in CRHP.

**Table 1**
Equations used to model the CRHP.

| |
|---|
| $T_1 = [T_{cw} - \Delta T_{driving}]$ |
| $T_3 = [T_{cw} + \Delta T_{driving}]$ |
| $P_2, P_3, h_3, h_4 = f(T_3, q = 0)$ |
| $T_2, h_2 = f(P_3, q = 1)$ |
| $h_1, s_1 = f(P_1, T_1)$ |
| $h_{2s} = f(P_3, s_1)$ |
| $h_2 = \frac{h_{2s} - h_1}{\eta_{is}} + h_1$ |

$NH_3$–$CO_2$–$H_2O$ systems and compares the performance of the two working fluid systems. Firstly, the thermodynamic models are discussed. Thereafter, the simple payback periods for these systems compared to a boiler are investigated where sensitivity analysis based on the electricity and gas prices is performed. The cost of $CO_2$ emission is, as well, taken into account.

## 2. Modelling approach

In its simplest form, CRHP consists of four main components: a compressor, a resorber, an expansion valve and a desorber (see Fig. 1). Various mixed working fluids can be used in CRHP, ideal candidates for HTHP are: $NH_3$–$H_2O$, or $NH_3$–$CO_2$–$H_2O$ (Gudjonsdottir et al., 2017), both zeotropic mixtures. Fig. 1 illustrates the case of a waste heat stream which is partly split up into two streams, where part of it is cooled down and the other part heated up. Hence, the waste heat stream can become available for both heating and cooling purposes. Of course, in practice this can also be two different streams at different temperature levels. In the following subsection the modeling approach for the compressor is described. A simplified model of the CRHP—similar to the one used by van de Bor et al. (2015) – is used to get initial guesses of the cycle variables to speed up the calculations. The main equations are listed in Table 1. In Section 3, two application cases are investigated. For the second case, to achieve more realistic pressure ratios, two compressors are used in series. The outlet of the first compressor is the inlet of the second one, and the pressure ratios are taken as equal so that the intermediate pressure is calculated with the following equation

$$P_{interm} = \sqrt{P_2 P_1} \tag{1}$$

The model assumes a fixed isentropic efficiency of the compressor, however, in reality it is a function of the cycle variables. As was shown by Gudjonsdottir et al. (2019) the difference can be significant depending on the operating conditions. Therefore, first an isentropic efficiency is assumed, then it is calculated with the compressor model and iterated until the efficiency change is within 0.1%. The following realistic assumptions are considered:

- Saturated liquid at the outlet of the resorber.
- Isenthalpic expansion.
- 5 K minimum temperature driving force in the resorber and desorber and no pressure drop.
- Mechanical efficiency of 0.90.

The coefficient of performance (COP) when only considering heating demands is defined as the ratio of the heat delivered and the energy required by the compressor (see Fig. 1 for reference states).

$$COP = \frac{h_2 - h_3}{h_2 - h_1} \tag{2}$$

When considering two compressors in series the required energy is the sum from the energy requirements of both compressors

$$COP_{2st} = \frac{h_2 - h_3}{(h_2 - h_{interm}) + (h_{interm} - h_1)} \tag{3}$$

When cooling demand is considered the COP is defined as the ratio of not only the heat delivered but additionally the cooling delivered and the energy required by the compressor

$$COP_{comb} = \frac{(h_2 - h_3) + (h_1 - h_4)}{h_2 - h_1} \tag{4}$$

### 2.1. The compressor model

The compressor calculations are based on the approach developed by Gudmundsdottir (2018). Since it can be challenging acquiring detailed geometry data from compressor manufacturers her approach was to scale the volume and area curves (port and leakage areas) from Tang (1995) and Zaytsev (2003) to a specific volumetric capacity. The main geometrical characteristics that are used in this study are listed in Table 2. The thermodynamic model is a homogenous model based on mass and energy conservations similar to that of Zaytsev (2003). However, the solving method was simplified in a similar way to the approach of Chamoun et al. (2013). The mass conservation can be defined in the following way:

$$\frac{dP}{d\phi} = \frac{1}{\left(\frac{\delta v}{\delta P}\right)_{T,x}} \left[ \frac{v}{m} \left( \sum_{k=1}^{n} \left( \frac{dm_{out}}{d\phi} \right)_k - \sum_{k=1}^{n} \left( \frac{dm_{in}}{d\phi} \right)_k \right) + \frac{1}{m} \frac{dV}{d\phi} - \left( \frac{\delta v}{\delta T} \right)_{P,x} \frac{dT}{d\phi} \right] \tag{5}$$

**Table 2**
Main geometrical characteristic of the compressor used in this study.

| | |
|---|---|
| Maximum volume per cavity, $m^3$ | $6.04 \cdot 10^{-5}$ |
| Length of the compressor rotors, m | 0.337 |
| Rotational speed, rpm | 10,000 |
| Number of male rotor lobes | 5 |
| Number of female rotor lobes | 6 |
| Clearance, µm | 50 |
| Discharge opens at, Âº | 690 |
| Stop angle, Âº | 760 |
| Mechanical efficiency, % | 90 |

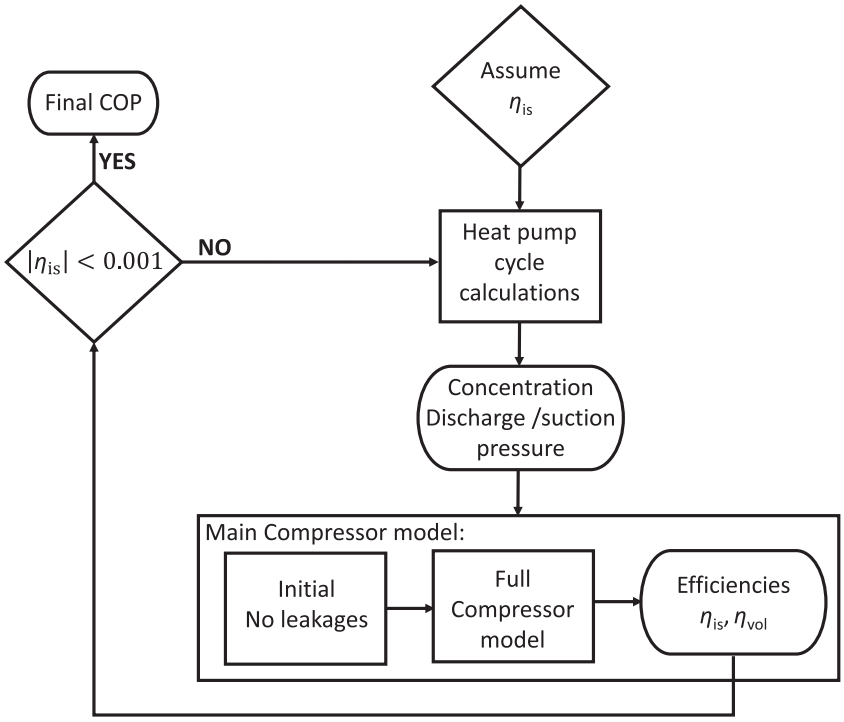


**Fig. 2.** Simplified flow chart of the integrated heat pump and compressor models.

And the energy conservation can be written in the following form:

$$\frac{dT}{d\phi} = \frac{T\left(\frac{\delta v}{\delta T}\right)_{P,x}\left[\frac{v}{m}\left(\sum_{k=1}^{n}\left(\frac{dm_{out}}{d\phi}\right)_k - \sum_{k=1}^{n}\left(\frac{dm_{in}}{d\phi}\right)_k\right) + \frac{1}{m}\frac{dV}{d\phi}\right]}{\left(\frac{\delta v}{\delta P}\right)_{T,x}\left(\frac{\delta h}{\delta T}\right)_{P,x} + T\left(\frac{\delta v}{\delta T}\right)^2_{P,x}} + \frac{\frac{\delta Q}{\delta \phi} + \sum_{k=1}^{l}(h_{in,k} - h)\left(\frac{dm_{in}}{d\phi}\right)_k}{m\left(\frac{\delta h}{\delta T}\right)_{P,x} + \frac{mT}{\left(\frac{\delta v}{\delta P}\right)_{T,x}}\left(\frac{\delta v}{\delta T}\right)^2_{P,x}} \tag{6}$$

The model takes into account the main leakage paths in a screw compressor, which are through:

- The contact line between the two rotors.
- The sealing line between the tip of the rotors and the housing.
- The cusp blowholes at compression side with high pressure.
- The compression-start blowholes at the suction side.
- The discharge end clearance.

Initially, the compression process is solved without any leakages and then including the main leakages. The iteration goes on until the difference in the pressure of each iteration step at 530 °, during the compression process, converges to a value with less than 1 Pa difference.

The model is implemented in Matlab. When operating with $NH_3$–$H_2O$ the thermodynamic properties are calculated with the method developed by Rattner and Garimella (2015). The compressor model was adapted to work with $NH_3$–$CO_2$–$H_2O$ as well by Gruijthuijsen (2019). In that case the thermodynamic properties are implemented in table form from the new fit developed by Gudjonsdottir et al. (2017).

The main results of the compressor model are the isentropic efficiency, the total isentropic efficiency (which includes the mechanical losses) and the volumetric efficiency. The enthalpy at the outlet of the compressor is obtained making use of the total isentropic efficiency in the equation given in Table 1. This assumes that the mechanical losses are added to the process side of the compressor. The volumetric efficiency allows to determine the required compressor size. The rotational speed is as given in Table 2.

Fig. 2 gives a schematic representation of the iteration process to identify the isentropic efficiency of the compressor as a function of the imposed external operating conditions. The solution concentration at the compressor inlet and the suction and discharge conditions imposed by the cycle model are the inputs to the compressor model which makes use of the solution properties, the compressor volume curve and the size and location of ports and leakage areas.

### 2.2. Economic calculations

To determine the simple payback time the methodology is adapted from Jensen et al. (2015). The payback time is calculated based on a CRHP replacing a gas burner:

$$PBP = \frac{TCI_{HP}}{(FC_{NG} - FC_{HP}) + (OMC_{NG} - OMC_{HP}) \cdot CRF} \tag{7}$$

Where the total cost of investment is determined as

$$TCI_{HP} = \sum_{k=1}^{K} PEC_k \cdot 3.11 \tag{8}$$

Where the factor 3.11, the same as used by van de Bor and Infante Ferreira (2013), accounts for additional cost such as installation. And the cost of each component is determined as

$$PEC_Y = PEC_W\left(\frac{X_Y}{X_W}\right)^{\gamma} \tag{9}$$

Where the $PEC_W$ is the cost at base capacity $X_W$ and $\gamma$ is the cost function exponent. In Table 3, an overview of the cost correlations for each equipment are given. The heat exchanger geometry from Jensen et al. (2015) is used and also their cost correlation for a low pressure ammonia chevron plate heat exchanger. From the thermodynamic calculations the necessary area is obtained. For the compressor the same correlation is also used, however, it is multiplied

**Table 3**
Cost correlations for the heat exchangers and compressor (Jensen et al., 2015).

| Equipment | $PEC_W$ (€) | $X_W$ | $\gamma$ |
|---|---|---|---|
| Heat exchangers | 15,526 | 42.0 [$m^2$] | 0.8 |
| Compressor | 11,914 · 2 | 178.4 [$m^3h^{-1}$] | 0.66 |
| Electrical motor | 10,710 · 2 | 250 [kW] | 0.65 |

by a factor of 2 to take into account the use of oil-free compressors instead of oil lubricated ones. The factor 2 was advised by industrial partners of the project.

The annual cost for the fuel consumption is estimated for the heat pump as

$$FC_{HP} = \frac{\dot{Q}}{COP}(c_{el} + c_{CO_2,el})H \tag{10}$$

Where $H$ is the total operating hours per year, $c_{el}$ is the cost of electricity and $c_{CO_2,el}$ is the cost of $CO_2$ emissions, which is estimated from the $CO_2$ emission factor for electricity and the cost of $CO_2$ emissions per ton. Similarly, the fuel cost per year is estimated for natural gas as:

$$FC_{NG} = \frac{\dot{Q}}{\eta_{NG}}(c_{NG} + c_{CO_2,NG})H \tag{11}$$

Both the cost of electricity and natural gas are varied depending on the predictions made by ECN (2017) for the Netherlands in 2020 to 2035. The $CO_2$ emission factor for natural gas is based upon the values for the Groningen gas field in the Netherlands (PBL, 2009) and the electricity factor is based up on the value from 2010 which was based on the integral method as defined by Harmelink et al. (2012). Since then this factor has increased slightly since use of coal has increased in the Netherlands. However, in the near future the share of renewables will be increased, therefore, this value might give a good estimate for the coming years. If only renewables are used this factor is close to zero, for the Netherlands this will most likely not happen in the near future. The share of renewable energy in the Netherlands in 2035 is estimated as 27.6% by ECN (2017). These values are all location sensitive and will differ from country to country and should therefore be taken with caution.

The operation and maintenance cost ($OMC$) is calculated in the same way as by Jensen et al. (2015), that is assumed 20% of the total investment cost, and therefore 0 for the gas burner. The capital recovery factor, $CRF$, is calculated as

$$CRF = \frac{i^{eff}(1+i^{eff})^{LT}}{(1+i^{eff})^{LT} - 1} \tag{12}$$

Where the effective interest rate is

$$i^{eff} = \frac{1+i}{1+i_L} - 1 \tag{13}$$

Table 4 gives an overview of the parameters and the values used for the cost calculations.

## 3. Results and discussion

### 3.1. Application cases

As mentioned by Chamoun et al. (2013) large amount of waste heat at 80–90 °C is available in various industrial sectors where higher temperatures are needed, typically around 120–130 °C. This is partly confirmed by a market study conducted by Spoelstra et al. (2017) for the EU28 countries. For most of the applications researched by them the source temperature varies from 50 to 110 °C, and the sink from 70 to 170 °C. There are specifically quite a number of applications having a source temperature of approximately 60 °C and a sink of 140 °C. As remarked in the introduction, CRHP, are ideal for high temperature applications. The first type of application that is considered is, therefore, heating of a waste heat stream from 90 to 130 °C, called case 1 from now on. It is assumed in that case that the inlet of the compressor is at 85 °C. And the second application with a larger temperature increase, from 60 °C to 140 °C, called case 2. For both cases it is assumed that the heat source and sink have a linear glide as a function of the heat load, as is the case with pressurized water. For both cases the focus is on upgrading the heat sink. Therefore, for each set of operating conditions the desorber outlet temperatures will vary. The only restriction is that the temperature pinch is kept as 5 K. The results are as well limited to a minimum pressure of 0.3 bar and maximum of 30 bar. These limits are chosen since operating at lower or higher pressure levels requires specialized and more expensive equipment according to industrial sources. For the $NH_3$–$CO_2$–$H_2O$ the thermodynamic property model is not reliable above approximately 50 wt% $NH_3$ (Gudjonsdottir et al., 2017). Therefore, the results with added $CO_2$ are only calculated until that limit.

The thermodynamic performance of both cases are presented first in the following section and in the subsequent section the economic results. All results are presented as a function of the $NH_3$ concentration. This is due to the reason that the mixture thermodynamic properties change significantly depending on the $NH_3$ concentration. It will be clear from the following sections that due to this change in properties the optimal thermodynamic case does not necessarily represent the optimum economic one.

### 3.2. Thermodynamic performance

When assuming a fixed isentropic efficiency of the compressor it was shown by van de Bor et al. (2014) for over 50 industrial cases that the ideal configuration for CRHP is to have close to saturated conditions at the compressor outlet. However, when taking

**Table 4**
Parameters used for the cost calculations and sources.

| Parameter | Sign | Value | Source |
|---|---|---|---|
| Interest rate | $i$ | 7% | (Jensen et al., 2015) |
| Inflation rate | $i_L$ | 2% | (Jensen et al., 2015) |
| Technical lifetime | $LT$ | 15 years | (Jensen et al., 2015) |
| Operating time | $H$ | 8600 h $year^{-1}$ | Industrial sources |
| Gas burner efficiency | $\eta_{NG}$ | 0.9 | (Jensen et al., 2015) |
| Electricity price | $c_{el}$ | 0.03–0.05 € $kWh^{-1}$ | (ECN, 2017) |
| Average electricity price (reference case) | $c_{el,\ avg}$ | 0.04 € $kWh^{-1}$ | |
| Natural gas price | $c_{NG}$ | 0.0134–0.034 € $kWh^{-1}$ | (ECN, 2017) |
| Average natural gas price (reference case) | $c_{NG,\ avg}$ | 0.0237 € $kWh^{-1}$ | |
| $CO_2$ price | $c_{CO_2}$ | 25 € $ton^{-1}$ | (EUA, 2019)* |
| $CO_2$ electricity emission factor | $c_{CO_2,el}$ | 0.460 kg $kWh^{-1}$ | (Harmelink et al., 2012) |
| $CO_2$ natural gas emission factor | $c_{CO_2,NG}$ | 0.202 kg $kWh^{-1}$ | (PBL, 2009) |

* Based on values from May, 2019

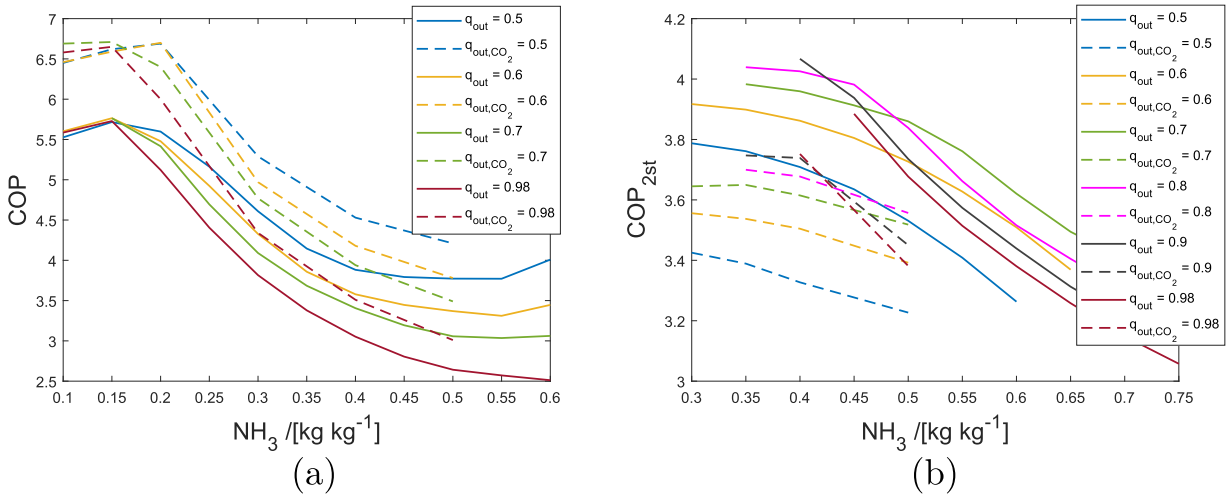


**Fig. 3.** COP as a function of the $NH_3$ concentration for various compressor outlet vapor qualities when a waste heat stream is heated from 90 to 130 °C (a) and from 60 to 140 °C (b). The solid lines are the results for $NH_3$–$H_2O$ and the dotted lines with added 5 wt% $CO_2$.

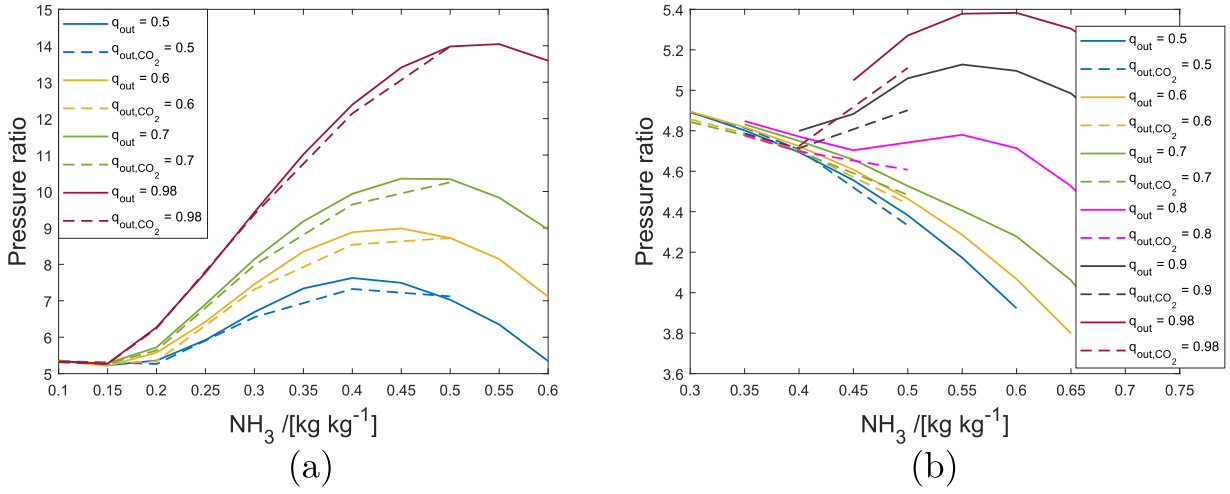


**Fig. 4.** Pressure ratio as a function the $NH_3$ concentration for various compressor outlet vapor qualities when a waste heat stream is heated from 90 to 130 °C (a) and from 60 to 140 °C (b).The solid lines are the results for $NH_3$–$H_2O$ and the dotted lines with added 5 wt% $CO_2$.

into account operating condition dependent compressor efficiency the outcome can be quite different. Even though twin screw compressors, as assumed in this case, can handle quite some liquid there is a limit. Therefore, the minimum outlet vapor quality is kept as 0.5. To make sure that no superheating occurs the highest tested vapor quality is kept at 0.98, instead of 1. In Fig. 3 the COP is shown as a function of the $NH_3$ concentration for various compressor outlet vapor qualities for both cases, and in Figs. 4 and 5 the pressure ratio and isentropic efficiency, respectively. The solid lines are the results for $NH_3$–$H_2O$ and the dotted lines with added 5 wt% $CO_2$. For case 2, using a single compressor results in pressure ratios in the range of 10–20. Therefore, as mentioned in the model section, two compressors in series are utilized for case 2. In that case the isentropic efficiencies, shown in Fig. 5, are the average from both compressors. The results for each compressor vary slightly, in the range of 1–2%.

It is clear that the thermodynamic performance differs significantly for the two cases. For case 1, the lower the outlet quality the higher the isentropic efficiency and as well the COP. In this case the thermodynamic optimum is when the resorber temperature glide is fit as closely as possible to the heat sink, that happens at low $NH_3$ concentrations or around 0.15–0.2 kg $kg^{-1}$, depending on the vapor quality. With 5 wt% added $CO_2$ the pressure ratio is slightly lower and both the isentropic efficiency and the COP increase. For case 2, a similar trend is seen with the added $CO_2$ concerning the isentropic efficiency and the pressure ratio, however, the COP decreases. In case 2, the temperature glide in the resorber is much larger, 80 K instead of 40 K. With the added $CO_2$ the temperature glide of the mixture decreases, this is beneficial in the first case, however, in the second case this has negative effects. The same reason is why there is a limit to the increase in COP with decreased vapor quality. By lowering the vapor quality the temperature glide of the mixture decreases as well, resulting at some point in lower COP (see Fig. 3). For this case the optimum when considering the $NH_3$ concentration is also higher, for the same reason. At higher concentrations, up to a certain limit (ca. 50 wt% $NH_3$), the temperature glide increases. Therefore, to get a good fit in the resorber higher ammonia concentrations are needed in case 2 than in case 1. In this case the highest COPs are around 0.35–0.4 wt% $NH_3$. Note that where the lines are cut off is where the pressure is lower than 0.3 bar or higher than 30 bar.

Above the main focus was on the heat sink. And in case 1 the heat source was cooled down from 90 °C to 60–80 °C, depending on the concentration. Those temperature levels are still too high for traditional cooling applications. In case 2, however, for $NH_3$ concentrations above 0.5 kg $kg^{-1}$ the heat source is cooled down

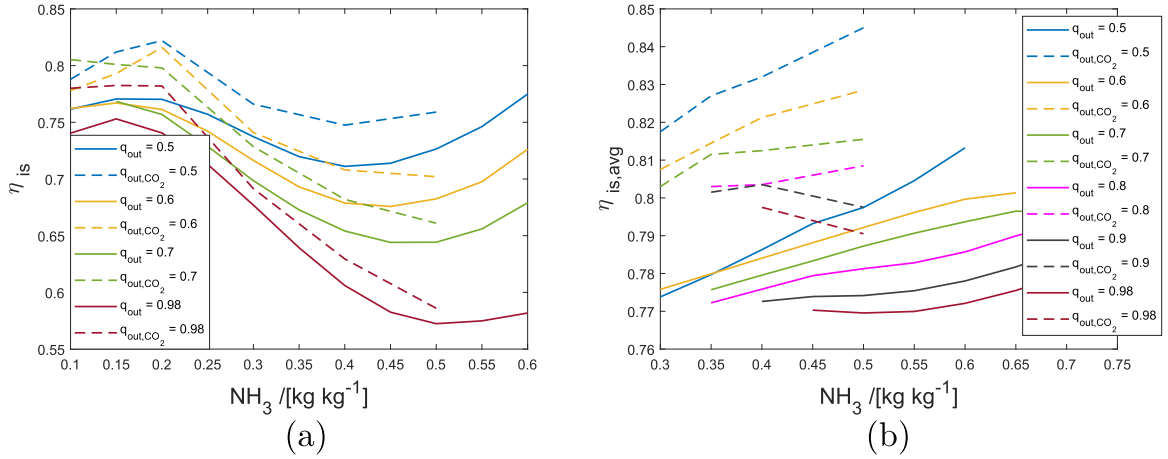


**Fig. 5.** $\eta_{is}$ as a function of the $NH_3$ concentration for various compressor outlet vapor qualities when a waste heat stream is heated from 90 to 130 °C (a) and from 60 to 140 °C (b).The solid lines are the results for $NH_3$–$H_2O$ and the dotted lines with added 5 wt% $CO_2$.

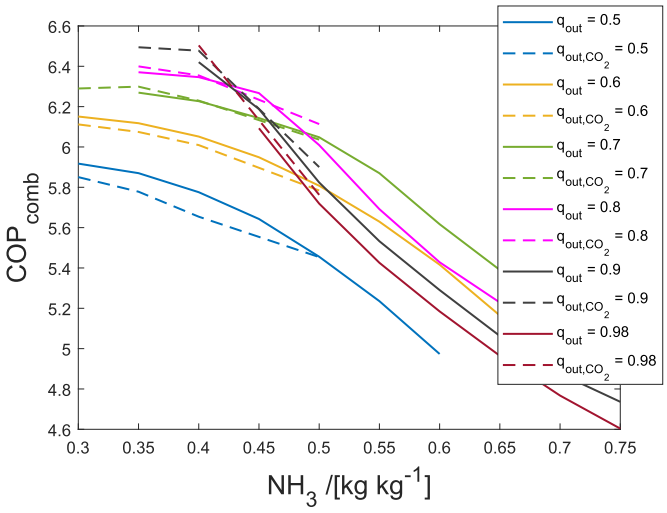


**Fig. 6.** $COP_{comb}$ as a function of $NH_3$ concentration for various compressor outlet vapor qualities when a waste heat stream is heated from 60 to 140 °C.The solid lines are the results for $NH_3$–$H_2O$ and the dotted lines with added 5 wt% $CO_2$.

to around 15 - 20 °C (assuming a temperature difference of 5 K in the desorber). These streams can be suitable for cooling if there are any cooling needs at the site. Therefore, additional benefits can be obtained using these concentrations. Fig. 6 shows the combined COP for case 2. In this case the COP with the added $CO_2$ is comparable or slightly lower than without. The difference in COP decreased mainly due to the benefits of the predicted increase in isentropic efficiency with the added $CO_2$.

### 3.3. Economic performance

In the report from Spoelstra et al. (2017) where 4065 potential heat pump installations were identified in the EU28 countries, the vast majority were found within thermal output of 10 MW. With many installations in the 1–2 MW range. Therefore, in the following analysis 1 MW, 5 MW and 10 MW installations are investigated. For case 2 only the $NH_3$–$H_2O$ mixture is considered since in that case the added $CO_2$ did not show any additional benefits. It should also be noted that it is assumed that the same components can be used for both mixtures. In reality specialized absorbers might be necessary when operating with the $NH_3$–$CO_2$–$H_2O$ mixture, as discussed by Gudjonsdottir (2020). Therefore, the $NH_3$–$CO_2$–$H_2O$ results should be taken with caution.

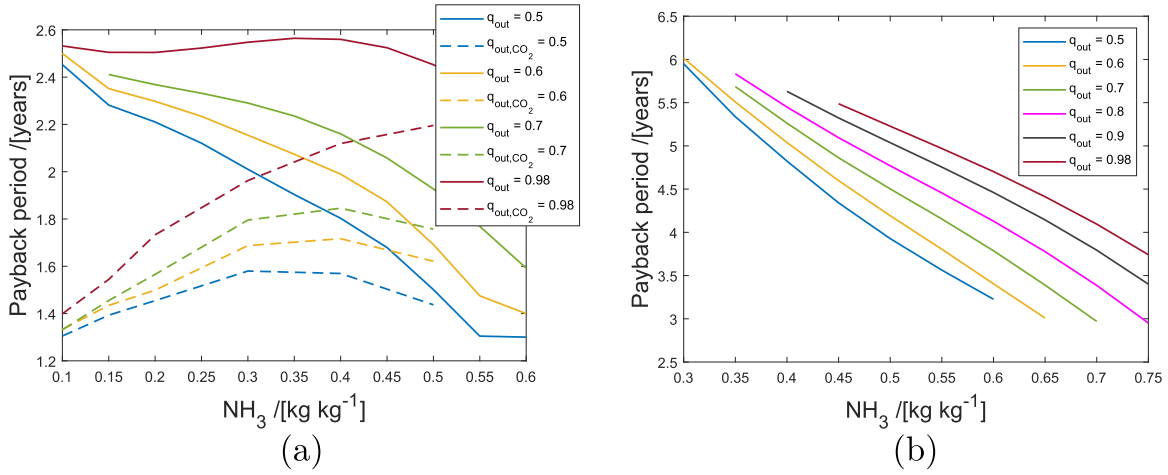


**Fig. 7.** The simple payback time taking the cost of $CO_2$ emissions into account as a function of the $NH_3$ concentration for various compressor outlet vapor qualities, assuming 1 MW thermal ouput, when a waste heat stream is heated from 90 to 130 °C (a) and from 60 to 140 °C (b). The solid lines are the results for $NH_3$-$H_2O$ and the dotted lines with added 5 wt% $CO_2$.

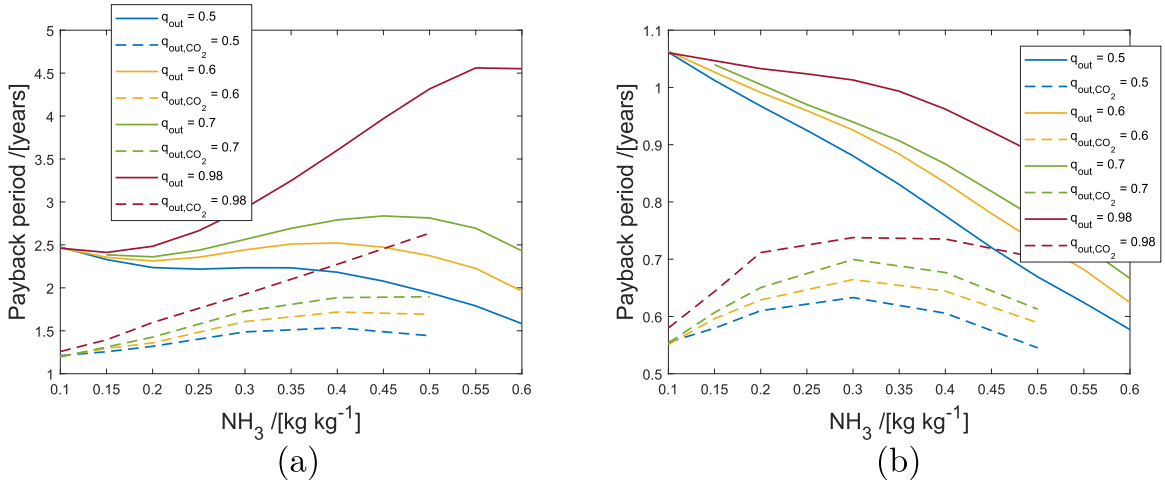


**Fig. 8.** The simple payback time taking the cost of $CO_2$ emissions into account as a function of the $NH_3$ concentration for various compressor outlet vapor qualities, assuming 5 MW thermal output, when a waste heat stream is heated from 90 to 130 °C. Assuming maximum electricity price and minimum natural gas price (a), and reversed, minimum electricity price and maximum natural gas price (b). The solid lines are the results for $NH_3$–$H_2O$ and the dotted lines with added 5 wt% $CO_2$.

Fig. 7 shows the simple payback time for the average electricity and gas price from Table 4 and 1 MW thermal output. Note that in the figure the price of $CO_2$ emissions is included. When it isn't included the payback periods are more or less twice as long. This shows that it is crucial to account for the cost of $CO_2$ emissions. When Fig. 7 is compared to Fig. 3 from the previous section, it is quite clear that the optimum thermodynamic performance is far from being the optimum economic one, especially what concerns the $NH_3$ concentration. In both cases the optimum thermodynamic performance is at much lower $NH_3$ concentration than the optimum economic one.

For case 1, the payback period decreases with decreased vapor quality. For the $NH_3$–$H_2O$ mixture, the payback period in general decreases with increased $NH_3$ concentration. This is mainly due to the fact that with increased $NH_3$ concentration a smaller compressor is needed since the density increases. With the added $CO_2$ the trend is slightly different, this is mostly due to the very high COPs at low $NH_3$ concentrations. The increase in density at higher concentrations is, therefore, not sufficient to decrease the payback period as much. For outlet compressor quality of 0.98 the trend is slightly different. In that case the pressure ratio and efficiency are too unfavorable at higher concentrations, due to a poor temperature fit in the resorber and high compressor outlet temperatures for higher concentrations. For case 2, these trends are even more prominent, that is the payback periods decrease with increased $NH_3$ concentration and decreased vapor quality. Similar results are seen for 5 and 10 MW thermal output with decreasing specific cost for increased capacity. For case 1 the minimum payback period decreases from approximately 1.3 years to 0.8 and 0.62 years for 5 and 10 MW thermal output, respectively, and from around 3 years to 1.8 and 1.4 years for case 2. In Fig. 8 the 5 MW case is shown when the extremes in electricity and natural gas price are assumed. That is on the left-hand side the maximum electricity price and the minimum natural gas price from Table 4 are used and reversed for the right-hand side. As can be seen from the figure the trends are slightly different, however, again with lower qualities and increased $NH_3$ concentrations, in general, the payback period decreases. In these instances the lowest payback periods are achieved with the added $CO_2$, again it is emphasized that it is assumed that similar equipment can be used as with $NH_3$–$H_2O$ which might not be the case. The optimal situation for heat pumps is, of course, when the natural gas price is at its maximum and the electricity price at its lowest point. However, even in the worst case scenario the lower payback periods are well within acceptable limits.

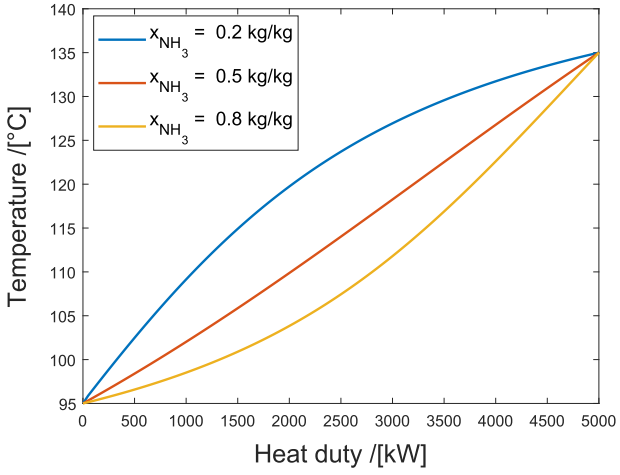


**Fig. 9.** Example temperature glides as a function of the heat load for $NH_3$ concentrations of 0.2 kg kg$^{-1}$, 0.5 kg kg$^{-1}$ and 0.8 kg kg$^{-1}$.

For case 2, the payback period is much longer as expected, since the COP is lower. However, as mentioned at the end of the last section, for this case there might be opportunities to use the heat source for cooling purposes. If that is the case, additional economical benefits can be obtained.

Tables 5 and 6 compare the cases that showed the best performance either thermodynamically or economically, assuming the average electricity and natural gas costs. Note that for case 2, where two compressors are used, the compressor cost and the motor cost is the combined cost for both compressors. Table 6 shows that the compressor is by far the most expensive component. The larger the volumetric flow (see Table 5), the larger compressor is needed. In this paper it is assumed that 10000 rpm is the maximum allowable speed for the compressor / drive under consideration. If a higher rotational speed would be feasible with the same drive arrangement, then it would be possible to increase the rotational speed and so the volumetric flow while the compressor costs remain comparable. The cost of the heat exchangers depend on their areas, which are closely linked to the temperature difference inside the heat exchangers. Fig. 9 shows examples

**Table 5**
Mixture composition, pressures, compressor inlet density, volumetric flow at the inlet of the compressor and COP results for the cases showing the best thermodynamic or economic performance.

| Case Nr. | $NH_3$ | (kg $kg^{-1}$) $H_2O$ | $CO_2$ | $q_{out}$ | $P_{low}$ (bar) | $P_{high}$ (bar) | $\rho_{comp,in}$ (kg $m^{-3}$) | $\dot{V}_{comp,in}$ ($m^3$ $s^{-1}$) | COP |
|---|---|---|---|---|---|---|---|---|---|
| 1 | 0.181 | 0.819 | 0 | 0.7 | 0.79 | 4.14 | 0.74 | 4.70 | 5.76 |
| 1 | 0.55 | 0.45 | 0 | 0.5 | 4.00 | 25.23 | 4.74 | 1.29 | 3.81 |
| 1 | 0.188 | 0.762 | 0.05 | 0.7 | 0.84 | 4.39 | 0.91 | 1.79 | 6.74 |
| 1 | 0.1 | 0.85 | 0.05 | 0.5 | 0.75 | 4.02 | 1.22 | 1.46 | 6.45 |
| 2 | 0.4 | 0.6 | 0 | 0.9 | 0.31 | 1.51 | 0.27 | 9.44 | 4.07 |
| 2 | 0.65 | 0.35 | 0 | 0.6 | 1.88 | 27.1 | 2.05 | 2.47 | 3.37 |

**Table 6**
Mixture composition, component cost (without installation cost) and the average simple payback time (assuming 5 MW thermal output) for the cases showing the best thermodynamic or economic performance.

| Case Nr. | $NH_3$ | (kg $kg^{-1}$) $H_2O$ | $CO_2$ | $PEC_{res}$ (k€) | $PEC_{des}$ (k€) | $PEC_{comp}$ (k€) | $PEC_{motor}$ (k€) | $PBP_{avg}$(5 MW) (years) |
|---|---|---|---|---|---|---|---|---|
| 1 | 0.181 | 0.819 | 0 | 45.0 | 58.9 | 481 | 48.1 | 1.50 |
| 1 | 0.55 | 0.45 | 0 | 44.9 | 65.7 | 205 | 63.0 | 0.77 |
| 1 | 0.188 | 0.762 | 0.05 | 47.7 | 60.0 | 255 | 43 | 0.90 |
| 1 | 0.1 | 0.85 | 0.05 | 34.6 | 57.5 | 222 | 44.7 | 0.78 |
| 2 | 0.4 | 0.6 | 0 | 34.8 | 33.7 | 1069 | 76.8 | 3.15 |
| 2 | 0.65 | 0.35 | 0 | 47.2 | 40.0 | 455 | 86.8 | 1.75 |

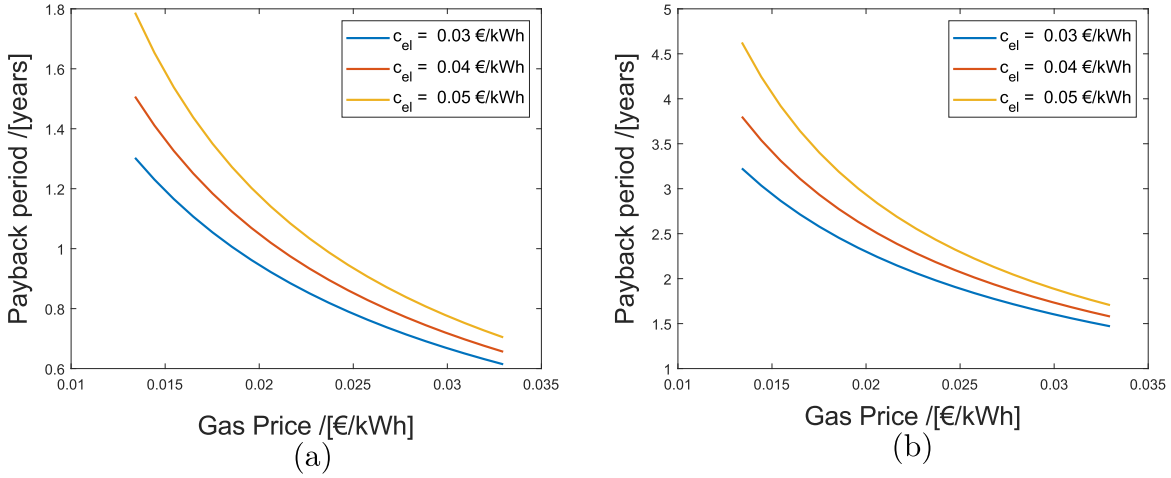


**Fig. 10.** The simple payback period of $NH_3$–$H_2O$ CRHPs, assuming 5 MW thermal output, as a function of the gas and electricity price for a compressor outlet vapor quality of 0.5 and $NH_3$ concentration of 0.55, when waste heat stream is heated from 90 to 130 °C (a) and for a compressor outlet vapor quality of 0.6 and $NH_3$ concentration of 0.65, when waste heat stream is heated from 60 to 140 °C (b).

of temperature glides for different $NH_3$ concentrations. For concentrations around 0.5 kg $kg^{-1}$ the glide most closely follows the glide of pressurized water (that is linear as a function of the heat load). In those cases larger and, therefore, slightly more expensive heat exchangers are needed than when the temperature fit is poorer.

From Tables 5 and 6 it is again very clear that there is a large difference between the best thermodynamic and economic case when it concerns the mixture concentrations. For the $NH_3$–$H_2O$ mixture and the highest energy performance, for the lower temperature glide, the optimum $NH_3$ concentration is about 0.2 kg $kg^{-1}$, while for the higher temperature glide the optimum $NH_3$ concentration is about 0.4 kg $kg^{-1}$. For the lowest payback time, for the lower temperature glide, the optimum $NH_3$ concentration is about 0.55 kg $kg^{-1}$ while for the higher temperature glide the optimum $NH_3$ concentration is about 0.65 kg $kg^{-1}$. For the ternary mixture the temperature glide of 80 K leads to unacceptable energy performance while for a temperature glide of 40 K a concentration of 0.15 kg $kg^{-1}$ $NH_3$, 0.05 kg $kg^{-1}$ $CO_2$ and 0.8 kg $kg^{-1}$ $H_2O$ leads to significant COP advantage in comparison to the binary mixture. For this temperature glide the best economic performance is obtained with a concentration of 0.1 kg $kg^{-1}$ $NH_3$, 0.05 kg $kg^{-1}$ $CO_2$ and 0.85 kg $kg^{-1}$ $H_2O$. The payback time is then comparable to the payback time of the binary mixture.

Fig. 10 shows, on the left hand side, the simple payback time results of $NH_3$-$H_2O$ for vapor outlet quality of 0.5 and $NH_3$ concentration of 0.55 for 5 MW thermal output for case 1 as a function of the gas and electricity price. The same figure, on the right hand side, shows similar result, however, for case 2. In this case the vapor quality is chosen as 0.6 and $NH_3$ concentration of 0.65 for 5 MW thermal output. It is clear in both cases that the payback time is highly sensitive to those prices, especially the gas price. The gas price has been predicted to rise in the following years according the study done by ECN (ECN, 2017). If this holds true the business case for CRHP will keep on improving. It is not shown in these figures, however, if the $CO_2$ emissions price is not taken into account the pay back times can be up to 8 times higher, depending on the electricity and gas price.

## 4. Conclusions

It is clear that CRHP are a very promising option to upgrade waste heat streams. This study shows that the payback period can very well be within acceptable limits, even for large temperature glides of 80 K. The results are, however, highly sensitive to the gas, electricity and $CO_2$ emission price as expected. It is also quite clear from the results that the thermodynamic optimum is far from being the most economical option in most cases. In general the following conclusions can be drawn from the results:

- The thermodynamic optimum depends on the temperature fit of the resorber when only focusing on heating applications for CRHP.
- It is crucial to account for the price of $CO_2$ emissions when investigating the business case for heat pumps.
- In general the simple payback period decreases with decreased vapor quality and increased $NH_3$ concentration.
- For CRHP the compressor is by far the most expensive component of the heat pump system.
- It depends on the application case if it is beneficial to use $NH_3$–$H_2O$ or $NH_3$–$CO_2$–$H_2O$ mixture as a working fluid for CRHP. If the temperature glide is very high, as it is for case 2 investigated in this study, then no additional benefits are attained from the added $CO_2$. For lower temperature glides, added $CO_2$ can increase the thermodynamic performance significantly, however, the economic advantages are limited. Quantitative results will depend on each specific application.

## Declaration of Competing Interest

The authors declare that they have no known competing financial interests or personal relationships that could have appeared to influence the work reported in this paper.

## Acknowledgments

The authors would like to thank the members of the ISPT "Upgrading waste heat streams with compression resorption heat pumps" project for their financial and in kind contributions. This project was supported by the following organizations: ISPT, TU Delft, DOW, Nouryon, Atlas Copco, IBK, Frames. This project received funding from TKI E&I with the supplementary grant 'TKI-Toeslag' for Topconsortia for Knowledge and Innovation (TKI's) of the Ministry of Economic Affairs and Climate Policy.

## References

Arpagaus, C., Bless, F., Schiffmann, J., Bertsch, S.S., 2016. Multi-temperature heat pumps: a literature review. Int. J. Refrig. 69, 437–465.
Arpagaus, C., Bless, F., Uhlmann, M., Schiffmann, J., Bertsch, S.S., 2018. High temperature heat pumps : market overview, state of the art, research status, refrigerants, and application potentials. Energy 152, 985–1010.
Bamigbetan, O., Eikevik, T.M., Nekså, P., Bantle, M., 2017. Review of vapour compression heat pumps for high temperature heating using natural working fluids. Int. J. Refrig. 80, 197–211.
Cao, F., Gao, T., Li, S., Xing, Z., Shu, P., 2011. Experimental analysis of pressure distribution in a twin screw compressor for multiphase duties. Exp. Therm Fluid Sci. 35, 219–225.
Chamoun, M., Rulliere, R., Haberschill, P., Peureux, J., 2013. Modelica-based modeling and simulation of a twin screw compressor for heat pump applications. Appl Therm Eng. 58, 479–489.
ECN, 2017. Nationale energieverkenning 2017. Technical report, Amsterdam/Petten, Netherlands.
EUA, 2019. Eu emission allowances | secondary market.Retrieved, 22nd of May 2019 from https://www.eex.com/en/market-data/environmental-markets/spot-market/eu-ropean-emission-allowances#!/2019/05/22.
Fukuda, S., Kondou, C., Takata, N., Koyama, S., 2014. Low GWP refrigerants R1234-ze(e) and R1234ze(z) for high temperature heat pumps. Int. J. Refrig. 40, 161–173.
Gruijthuijsen, D. A. W., 2019. Development of a wet screw compressor model operating with $NH_3$-$CO_2$-$H_2O$. Master thesis, Delft University of Technology.
Gudjonsdottir, V., 2020. Upgrading waste heat streams with wet compression. PhD thesis, Delft University of Technology.
Gudjonsdottir, V., Infante Ferreira, C.A., Goethals, A., 2019. Wet compression model for entropy production minimization. Appl. Therm. Eng. 149, 439–447.
Gudjonsdottir, V., Infante Ferreira, C.A., Rexwinkel, G., Kiss, A.A., 2017. Enhanced performance of wet compression-resorption heat pumps by using $NH_3$-$CO_2$-$H_2$o as working fluid. Energy 124, 531–542.
Gudmundsdottir, K., 2018. Theoretical and experimental investigation of a wet compression process operating with ammonia-water in the application of a CRHP. Master thesis, Delft University of Technology.
Harmelink, M., Bosselaar, L., Gerdes, J., Boonekamp, P., Segers, R., Pouwelse, H., Verdonk, M., 2012. Berekening van de $CO_2$-emissies, het primair fossiel energiegebruik en het rendement van elektriciteit in Nederland. Technical report, the Netherlands.
IEA, 2014. Application of industrial heat pumps. Technical report. https://www.energiteknologi.dk/sites/energiteknologi.dk/files/slutrapporter/annex_xiii_part_a.pdf.
Jensen, J.K., Ommen, T., Markussen, W.B., Reinholdt, L., Elmegaard, B., 2015. Technical and economic working domains of industrial heat pumps: part 2 - Ammonia-water hybrid absorption-compression heat pumps. Int. J. Refrig 5, 183–200.
Kiss, A.A., Infante Ferreira, C.A., 2016. Heat Pumps in Chemical Process Industry. CRC-Press (Taylor & Francis Group), US.
Kondou, C., Koyama, S., 2015. Thermodynamic assessment of high-temperature heat pumps using low-GWP HFO refrigerants for heat recovery. Int. J. Refrig. 53, 126–141.
Król, J., Oclon, P., 2019. Sensitivity analysis of hybrid combined heat and power plant on fuel and $CO_2$ emission allowances price change. Energy Convers. Manag. 196, 127–148.
Mikielewicze, O., Wajs, J., 2019. Performance of the very high-temperature heat pump with low GWP working fluids. Energy 182, 460–470.
PBL, 2009. Uncertainty in the Netherlands'Greenhouse Gas Emissions Inventory: Estimation of the Level and Trend Uncertainty Using the IPCC Tier 1 Approach. Technical report, Bilthoven, the Netherlands.
Rattner, A.S., Garimella, S., 2015. Fast, stable computation of thermodynamic properties of ammonia-water mixtures. Int. J. Refrig. 62, 39–59.
Shen, J., Xing, Z., Zhang, K., He, Z., Wang, X., 2016. Development of a water-injected twin-screw compressor for mechanical vapor compression desalination systems. Appl. Therm. Eng. 95, 125–135.
Spoelstra, S., Wemmers, A., Groen, R., 2017. Dutch program for the Acceleration of sustainable Heat Management in industry, Scoping study final report.
Tang, Y., 1995. Computer aided Design of Twin Screw Compressors.PhD thesis, University of Strathclyde.
Tian, Y., Yuan, H., Wang, C., Wu, H., Xing, Z., 2017. Numerical investigation on mass and heat transfer in an ammonia oil-free twin-screw compressor with liquid injection. Int. J. Therm. Sci. 120, 175–184.
van de Bor, D.M., Infante Ferreira, C.A., 2013. Quick selection of industrial heat pump types including the impact of thermodynamic losses. Energy 53, 312–322.
van de Bor, D.M., Infante Ferreira, C.A., Kiss, A.A., 2014. Optimal performance of compression-resorption heat pump systems.. Appl. Therm. Eng. 65, 219–225.
van de Bor, D.M., Infante Ferreira, C.A., Kiss, A.A., 2015. Low grade waste heat recovery using heat pumps and power cycles. Energy 89, 864–873.
Xiaohui, Y., Yufeng, Z., Na, D., Chengmin, C., Lijun, M., Lipin, D., Yan, Z., 2014. Experimental performance of high temperature heat pump with near-azeotropic refrigerant mixture. Energy Build. 78, 43–49.
Zaytsev, D., 2003. Development of Wet Compressor for Application in Compression-Resorption Heat Pumps. PhD thesis, Delft University of Technology.
Zhang, J., Zhang, H., He, Y., Tao, W., 2016. A comprehensive review on advances and applications of industrial heat pumps based on the practices in china. Appl. Energy 178, 800–825.
Zhang, Y., Zhang, Y., Yu, X., Guo, J., Deng, N., Dong, S., He, Z., Ma, X., 2017. Analysis of a high temperature heat pump using BY-5 as refrigerant. Appl. Therm. Eng. 127, 1461–1468.